Naval Research Laboratory
Washington, DC 20375-5320

NRL/MR/6790--99-8321

Propagation of Short Laser Pulses in Plasma Channels

P. Sprangle

Beam Physics Branch
Plasma Physics Division

B. Hafizi

Icarus Research, Inc.
Bethesda, Maryland

P. Serafim

Northeastern University
Department of Electrical Engineering
Boston, Massachusetts

March 2, 1999

REPORT DOCUMENTATION PAGE

Form Approved
OMB No. 0704-0188

1. AGENCY USE ONLY (*Leave Blank*)	2. REPORT DATE	3. REPORT TYPE AND DATES COVERED
	March 2, 1999	Interim

4. TITLE AND SUBTITLE

Propagation of Short Laser Pulses in Plasma Channels

5. FUNDING NUMBERS

67-0899-09

6. AUTHOR(S)

P. Sprangle, B. Hafizi,† and P. Serafim‡

7. PERFORMING ORGANIZATION NAME(S) AND ADDRESS(ES)

Naval Research Laboratory
Washington, DC 20375-5320

8. PERFORMING ORGANIZATION REPORT NUMBER

NRL/MR/6790--99-8321

9. SPONSORING/MONITORING AGENCY NAME(S) AND ADDRESS(ES)

Office of Naval Research
800 North Quincy Street
Arlington, VA 22217-5660

U.S. Department of Energy
Washington, DC 20585

10. SPONSORING/MONITORING AGENCY REPORT NUMBER

11. SUPPLEMENTARY NOTES

† Icarus Research, Inc.
P.O. Box 30780
Bethesda, MD 20824-0780

‡ Northeastern University
Department of Electrical Engineering
Boston, MA 02115

12a. DISTRIBUTION/AVAILABILITY STATEMENT

Approved for public release; distribution unlimited.

12b. DISTRIBUTION CODE

13. ABSTRACT (*Maximum 200 words*)

Finite pulse length effects are shown to play a major role in the propagation, stability and guiding of intense laser beams in plasmas. We present the quasi paraxial approximation (QPA) to the wave equation that takes finite pulse length effects into account. The QPA is an extension of the usual paraxial approximation. The laser field is shown to be significantly modified for pulses less than a few tens of wavelengths long. A pair of coupled envelope-power equations having finite pulse length effects, as well as relativistic and atomic electron nonlinearities, is derived and analyzed. Short laser pulses propagating in plasma channels are found to undergo an envelope oscillation in which the front of the pulse is always damped while the back initially grows. The modulation eventually damps due to frequency spread phase mixing. In addition, finite pulse length effects are shown to significantly modify nonlinear focusing processes.

14. SUBJECT TERMS

Intense laser pulses
Propagation
Plasma channels
Ultra-short pulses
Modulation instability

15. NUMBER OF PAGES

37

16. PRICE CODE

17. SECURITY CLASSIFICATION OF REPORT	18. SECURITY CLASSIFICATION OF THIS PAGE	19. SECURITY CLASSIFICATION OF ABSTRACT	20. LIMITATION OF ABSTRACT
UNCLASSIFIED	UNCLASSIFIED	UNCLASSIFIED	UL

NSN 7540-01-280-5500

Standard Form 298 (Rev. 2-89)
Prescribed by ANSI Std 239-18
298-102

CONTENTS

PROPAGATION OF SHORT LASER PULSES IN PLASMA CHANNELS

I. Introduction

Advances in laser technology have resulted in a new class of compact, ultrashort pulse lasers with extremely high intensities [1-3]. Intense pulses have numerous potential applications in areas such as advanced laser-driven accelerators [4-14], harmonic generators [15-19], x-ray lasers [20,21], other short wavelength radiation sources [22], and "fast ignitor" laser fusion [23-25]. Laser technology is now being pushed to such extremely short pulse lengths that the pulse is only a few optical cycles in duration. For example, at a wavelength of 0.8 μm, Barty [2] has produced pulses of 4 TW peak power with durations of 18 fs (~ 7 wavelengths) with plans to extend these results to ~ 10 fs and > 100 TW. In this regime, finite pulse length effects may play an important role in the laser pulse propagation dynamics.

The propagation dynamics of long laser pulses (long compared to the wavelength) is described by the well-known paraxial wave equation. In the paraxial wave equation approximation, lowest order diffraction effects associated with the laser beam are retained but finite pulse length and higher order diffraction effects are neglected. The solutions to the paraxial wave equation in vacuum are the well-known Laguerre-Gaussian functions that describe the dynamics of long laser beams [26]. When the laser pulse length becomes sufficiently short, i.e., less than ~ 10's of wavelengths, finite pulse length effects can play an important role [27]. An example of this is the propagation of short laser pulses in a guiding channel. Extended laser pulse propagation in a plasma channel [28-40] is important in a number of applications, including high gradient accelerators and x-ray lasers.

In this paper a quasi paraxial approximation (QPA) is introduced which is an extension of the well-known paraxial approximation to the wave equation to include finite pulse length effects. Employing the QPA, a pair of coupled envelope-power equations is derived for short

Manuscript approved December 21, 1998.

laser pulses propagating in vacuum, plasma and channels. The model includes atomic electron and relativistic effects. The results contained in this paper include: i) an analytical formulation of short laser pulses using the QPA, ii) a derivation of a pair of coupled laser envelope-power equations, iii) a laser envelope modulation which eventually damps due to frequency spread phase mixing, iv) demonstration of significant modification of nonlinear processes due to finite pulse length effects, and v) analysis of short pulse propagation dynamics in long plasma channels. These results represent new features and effects associated with short pulse lasers. Short laser pulse effects have been considered numerically or in one dimension by others [41-44], however, the major findings in this paper were not addressed. For example, due to finite pulse length effects, the trailing edge of an unmatched laser pulse propagating in a plasma channel is found to undergo an envelope oscillation, while the leading edge is damped. For a sufficiently short pulse the modulation will modify the main body of the pulse. The laser envelope modulation is shown to be due to the dependence of the pulse group velocity on the spot size through the pulse length. In addition, finite pulse length effects are shown to significantly increase nonlinear focusing processes.

The organization of this paper is as follows. The general wave equation for the electric field of a finite length laser pulse propagating in vacuum, plasmas or channels, including nonlinear (atomic and relativistic) focusing effects, is presented and discussed in Sec. II. In Sec. III the propagation dynamics of a short pulse in vacuum or uniform plasma is derived. In Sec. IV a general pair of coupled envelope-power equation is derived. These equations are used to analyze the propagation of a short laser pulse in a preformed plasma channel with nonlinear focusing effects. Various propagation limits are discussed and the laser envelope modulation is analyzed. The laser envelope modulation is discussed in Sec. V. Numerical illustrations are

presented in Sec. VI and a conclusion is given in Sec. VII. In the Appendix the range of validity of the QPA is obtained in two limiting cases.

II. Finite Pulse Length Model

The propagation medium is a vacuum, plasma or preformed plasma channel consisting of free and bound electrons, i.e., partially stripped plasma. Nonlinear processes arising from relativistic and atomic polarization effects are included. The wave equation includes a plasma current consisting of free electrons and a polarization current arising from the bound atomic electrons and is given by [31,45,46],

$$\left(\nabla_{\perp}^2 + \frac{\partial^2}{\partial z^2} - c^{-2}\,\frac{\partial^2}{\partial t^2}\right)\mathbf{E} = 4\pi c^{-2}\left(\frac{\partial \mathbf{J}_p}{\partial t} + \frac{\partial^2 \mathbf{P}}{\partial t^2}\right), \tag{1}$$

where $\nabla_{\perp}^2$ is the transverse Laplacian, $\mathbf{E}(\mathbf{r},t)$ is the electric field, $\mathbf{J}_p$ is the plasma current density associated with the free electrons and $\mathbf{P}$ is the polarization field associated with the bound electrons. The atomic polarization field consists of a linear and nonlinear part, $\mathbf{P} = (1/4\pi)(\eta_0^2 - 1 + 2\eta_0\eta_2 I)\mathbf{E}$, where η_0 is the linear index, η_2 is the nonlinear refractive index and $I = (c/4\pi)\eta_0 \langle \mathbf{E} \bullet \mathbf{E} \rangle$ is the time averaged laser intensity. In the present model, the origin of the nonlinear index η_2 is the anharmonic potential in which the bound electrons oscillate. Noting that $\partial \mathbf{J}_p / \partial t = (4\pi)^{-1}\omega_p^2(r)\mathbf{E}$ and setting $\eta_0 = 1$, the wave equation becomes

$$\left(\nabla_{\perp}^2 + \frac{\partial^2}{\partial z^2} - \frac{1}{c^2}\frac{\partial^2}{\partial t^2} - \frac{\omega_p^2(r)}{c^2} + \beta < \mathbf{E} \bullet \mathbf{E} >\right)\mathbf{E} = 0, \tag{2}$$

where $\omega_p(r) = (4\pi q^2 n_p(r)/m)^{1/2}$ is the plasma frequency and $n_p(r)$ is the plasma density. In Eq. (2) the coefficient of the nonlinear term $\beta = \beta_p + \beta_a$ denotes relativistic free electron effects as well as nonlinear atomic electron effects arising from η_2,

$$\beta_p = \frac{1}{2}\left(\frac{q}{mc^2}\right)^2\left(\frac{\omega_{p0}}{\omega}\right)^2, \tag{3a}$$

$$\beta_a = \frac{c}{2\pi}\frac{\omega^2}{c^2}\eta_2, \tag{3b}$$

where $\omega_{p0} = (4\pi q^2 n_{p0}/m)^{1/2}$, n_{p0} is the density on axis (r = 0), and ω is the characteristic laser frequency. In Eq. (3), β_p results in a critical power for relativistic focusing [31,47-50] while the β_a results in a critical power for atomic electron focusing [31,51-53]. In a partially stripped plasma, atomic effects can occur on a time scale ~ 10^{-15} sec and can dominate free electron effects in the nonlinear term [32,45,46]. The nonlinear term, due to relativistic free electrons, is only significant when the laser pulse length is longer than a plasma period [54]. The critical powers for relativistic focusing in plasma and nonlinear focusing in a gas are, respectively,

$$P_p = 2c(q/r_e)^2(\omega/\omega_p)^2, \tag{4a}$$

and

$$P_a = \lambda^2/(2\pi\eta_2), \tag{4b}$$

where r_e is the classical electron radius. In general, when the laser power exceeds either of these critical powers, focusing occurs [31,45,46]. The total nonlinear focusing power consists of contributions from both P_p and P_a and is given by

$$P_c = P_p P_a/(P_p + P_a). \tag{4c}$$

The preformed plasma density channel is taken to be a function of radial position in order to provide for guiding of the laser pulse. The radial dependence of the plasma frequency is given by

$$\omega_p(r) = \omega_{p0}\left(1 + \frac{\Delta n}{n_{p0}}\frac{r^2}{r_c^2}\right)^{1/2}, \tag{5}$$

where $n_{p0} + \Delta n$ is the density at the edge of the plasma channel ($r = r_c$). For guiding, the plasma density must increase as a function of r, i.e., $\Delta n > 0$.

Laser induced plasma waves, wakefields [55,56], are neglected. This can be justified if the laser pulse length is less than a plasma period or if the laser intensity is sufficiently low.

a) Quasi Paraxial Approximation (QPA) to Wave Equation

The laser electric field is of the form

$$\mathbf{E} = \mathbf{E}_0 \exp(i(kz - \omega t))/2 + c.c., \tag{6}$$

where $\mathbf{E}_0(\mathbf{r},t)$ is the complex amplitude, k is the wavenumber and ω is the frequency. Substituting Eqs. (5) and (6) into Eq. (2) gives the wave equation for $\mathbf{E}_0$,

$$\left[\nabla_\perp^2 + 2i\left(k\frac{\partial}{\partial z} + \frac{\omega}{c^2}\frac{\partial}{\partial t}\right) + \frac{\partial^2}{\partial z^2} - \frac{1}{c^2}\frac{\partial^2}{\partial t^2} - K_c^2\frac{r^2}{r_c^2} + \beta\,\mathbf{E}_0 \bullet \mathbf{E}_0^*/2\right]\mathbf{E}_0 = 0, \tag{7}$$

where $K_c = (\omega_{p0}/c)(\Delta n/n_{p0})^{1/2}$ is the focusing parameter associated with the plasma channel and we have set $k = \left(\omega^2/c^2 - \omega_{p0}^2/c^2\right)^{1/2}$. Changing variables from (z, t) to (z,ξ) where $\xi = z - \eta_p ct$, and setting $k = \eta_p\omega/c$, where $\eta_p = (1 - \omega_{p0}^2/\omega^2)^{1/2}$ is the linear on-axis plasma refractive index, Eq. (7) becomes

$$\left[\nabla_\perp^2 + 2i\eta_p \frac{\omega}{c}\frac{\partial}{\partial z} + 2\frac{\partial^2}{\partial z \partial \xi} + (1-\eta_p^2)\frac{\partial^2}{\partial \xi^2} + \frac{\partial^2}{\partial z^2} - K_c^2 \frac{r^2}{r_c^2} + \beta \mathbf{E}_0 \bullet \mathbf{E}_0^* / 2\right]\mathbf{E}_0 = 0. \quad (8)$$

The second term on the left-hand side of Eq. (8) represents first order diffraction effects, the third term denotes first order finite pulse effects, the fourth and fifth terms denote higher order finite pulse and diffraction effects respectively while the last two represent guiding and nonlinear focusing, respectively.

In the absence of channel guiding ($K_c = 0$) and nonlinear focusing ($\beta = 0$) we can obtain an estimate for the order of magnitude of the various terms in Eq. (8). The second, third, fourth and fifth terms in Eq. (8) are approximately of order

$$2\eta_p(\omega/c)\left|\partial/\partial z\right| \sim \frac{4}{r_0^2}, \quad (9a)$$

$$2\left|\frac{\partial^2}{\partial z \partial \xi}\right| \sim \left(\frac{1}{\pi\eta_p}\frac{\lambda}{\ell_0}\right)\frac{4}{r_0^2}, \quad (9b)$$

$$\left(1-\eta_p^2\right)\left|\frac{\partial^2}{\partial \xi^2}\right| \sim \left(\frac{r_0}{2\lambda}\frac{\omega_p}{\omega}\right)^2\left(\frac{\lambda}{\ell_0}\right)^2\frac{4}{r_0^2}, \quad (9c)$$

$$\left|\frac{\partial^2}{\partial z^2}\right| \sim \left(\frac{\lambda}{2\pi\eta_p r_0}\right)^2\frac{4}{r_0^2}, \quad (9d)$$

respectively, where r_0 and ℓ_0 are the spot size and pulse length. In obtaining the estimates in Eq. (9) we used $\left|\partial/\partial\xi\right| \sim 1/\ell_0$ and $\left|\partial/\partial z\right| \sim 1/Z_R$, where $Z_R = \pi\eta_p r_0^2/\lambda$ is the Rayleigh length in the plasma and λ is the vacuum wavelength. The relative order of magnitudes of the first, second, third, fourth and fifth terms in Eq. (8) is

$$1 \;:\; 1 \;:\; \frac{1}{\pi\eta_p}\frac{\lambda}{\ell_0} \;:\; \frac{1-\eta_p^2}{4\pi\eta_p}\frac{Z_R}{\ell_0}\frac{\lambda}{\ell_0} \;:\; \frac{1}{4\pi\eta_p}\frac{\lambda}{Z_R}. \quad (10)$$

The first two terms in the wave equation are comparable and lead to the paraxial wave equation approximation. In the paraxial approximation finite length effects and higher order diffraction are neglected, i.e., the third, fourth and fifth terms in Eq. (8) are neglected. The paraxial wave equation assumes that $\lambda/\ell_0 << 1$, $(1-\eta_p^2)(Z_R/\ell_0)\lambda/\ell_0 << 1$, and $\lambda/Z_R << 1$ and is given by

$$\left(\nabla_\perp^2 + 2i\eta_p \frac{\omega}{c}\frac{\partial}{\partial z}\right)\mathbf{E}_0 = 0. \tag{11}$$

Solutions of the paraxial wave equation are the well-known Laguerre-Gaussian functions [26].

When the Rayleigh length is large compared to the pulse length, $Z_R >> \ell_0$, the higher order diffraction term can be neglected compared to the finite pulse length terms resulting in the following wave equation

$$\left(\nabla_\perp^2 + 2i\eta_p \frac{\omega}{c}\left(1 - \frac{i}{\eta_p}\frac{c}{\omega}\frac{\partial}{\partial\xi}\right)\frac{\partial}{\partial z} + (1-\eta_p^2)\frac{\partial^2}{\partial\xi^2}\right)\mathbf{E}_0 = 0. \tag{12}$$

Equation (12) contains first order diffraction and finite pulse length effects and reduces to the paraxial equation, Eq. (11), when the pulse length is much longer than the wavelength, $\ell_0 >> \lambda$.

b) Finite Pulse Length Wave Equation

Finite pulse length effects are represented by the terms $\partial^2/\partial z\partial\xi$ and $\partial^2/\partial\xi^2$ in Eq. (12). These terms under certain conditions can be simplified using the QPA, allowing for the analytical solution for the field. To analyze finite pulse length effects we assume that the general solution of Eq. (12) for the fundamental transverse Gaussian complex amplitude is given by

$$\mathbf{E}_0 = b\exp\left[i\varphi - (1+i\theta)r^2/r_s^2\right]\hat{e}_\perp, \tag{13}$$

where b, φ, θ and r_s are real functions of z and $\xi = z - \eta_p ct$ and $\hat{e}_\perp$ is a unit transverse vector defining the polarization. In Eq. (13), b is the amplitude, φ is the phase, θ is related to the wavefront curvature, and r_s is the spot size of the laser pulse. The central assumption in the QPA is that the main contribution from the finite length term will come from the ξ dependence in the initial amplitude. Hence, we make the approximations $\partial \mathbf{E}_0 / \partial \xi \cong (\partial \ell n(b_0) / \partial \xi) \mathbf{E}_0$ and $\partial^2 \mathbf{E}_0 / \partial \xi^2 \cong \left(\partial^2 \ell n(b_0) / \partial \xi^2 + (\partial \ell n(b_0) \partial \xi)^2\right) \mathbf{E}_0$, where $b_0(\xi) = b(z = 0, \xi)$. In the Appendix the QPA will be shown to be well satisfied for a broad range of parameters. Employing the QPA, Eq. (12), including the guiding term and relativistic/atomic electron nonlinearities, becomes

$$\left[\nabla_\perp^2 + 2i\eta_p \frac{\omega}{c}(1 + i\varepsilon(\xi))\frac{\partial}{\partial z} - \frac{\omega^2}{c^2}\eta_p^2 (1 - \eta_p^2) g(\xi) - K_c^2 r^2 / r_c^2 + \beta \mathbf{E}_0 \bullet \mathbf{E}_0^* / 2\right] \mathbf{E}_0 = 0, \tag{14a}$$

where

$$\varepsilon(\xi) = \frac{-c}{\omega \eta_p} \frac{\partial \ell n(b_0(\xi))}{\partial \xi}, \tag{14b}$$

and

$$g(\xi) = \frac{c}{\omega \eta_p} \frac{\partial \varepsilon}{\partial \xi} - \varepsilon^2. \tag{14c}$$

Finite pulse length effects are represented by the functions ε(ξ) and g(ξ). If the laser pulse amplitude has an initial Gaussian longitudinal profile, ~ $\exp(-4\xi^2 / \ell_0^2)$, we find that

$$\varepsilon(\xi) = \frac{8c}{\omega \eta_p} \frac{\xi}{\ell_0^2} = \frac{4}{\pi \eta_p} \frac{\lambda \xi}{\ell_0^2}, \tag{15a}$$

and

$$g(\xi) = 2\left(\frac{\lambda}{\pi\eta_p \ell_0}\right)^2\left(1 - \frac{8\xi^2}{\ell_0^2}\right). \qquad (15b)$$

The functions ε and g have magnitudes much less than unity in the vicinity of the laser pulse, i.e., $|\xi| \lesssim \ell_0$. To estimate the order of magnitude for ε and g we take λ = 1 μm and ℓ_0 = 15 μm (50 fs pulse) and obtain $\varepsilon(\xi = \ell_0) = 8 \times 10^{-2}$ and $g(\xi = \ell_0) = -6 \times 10^{-3}$.

The quasi-paraxial wave equation, Eq. (14a), indicates that finite pulse length effects can be important when $\ell_0 < (\lambda/r_0)^2 L$, where L is the propagation length. This implies that finite pulse length effects are significant when $L >> Z_R$, as would be the case for a guided laser pulse.

The laser field, which is described by Eq. (13), depends on the functions b, φ, θ, and r_s. To obtain equations for b, φ, θ, and r_s, we substitute Eq. (13) into the wave equation, Eq. (14a), containing finite pulse length effects, plasma channel guiding and nonlinear focusing. Equating like powers of r leads to coupled equations for b, φ, θ, and r_s,[57]

$$Q + i(1+i\varepsilon)\frac{\partial}{\partial Z}\left[\frac{1}{2}\ell n(P/R^2) + i\varphi\right] + P/(2R^2) - \alpha = 0, \qquad (16a)$$

$$Q^2 + i(1+i\varepsilon)\frac{\partial}{\partial Z}Q - R_m^{-4} - \frac{P}{R^4} = 0, \qquad (16b)$$

where $Q(Z,\xi) = -(1 + i\theta)/R^2$, $R = r_s/r_0$ is the normalized spot size, r_0 is the initial spot size, $R_m = r_m/r_o$, $r_m = (2r_c/K_c)^{1/2}$, $\alpha(\xi) = (Z_R/r_0)^2(1-\eta_p^2)g(\xi)$, $Z_R = \eta_p \omega r_0^2/2c = \eta_p \pi r_0^2/\lambda$ is the Rayleigh length, $Z = z/Z_R$, $P(Z,\xi) = P_L(Z,\xi)/P_c$ is the laser power normalized to the nonlinear focusing power, $P_L(Z,\xi) = P_{peak}(b/\hat{b}_0)^2 R^2$ is the laser power, $\hat{b}_0$ is the peak amplitude at Z = 0, P_{peak} is the peak laser power at Z = 0 and P_c is the nonlinear focusing power in Eq. (4c) which can be due to both relativistic and atomic electron effects.

III. Short Pulse Propagation in Vacuum or Uniform Plasma

a) Fundamental Transverse Gaussian Pulse Solution

In this section we obtain and discuss the finite pulse length solution to Eq. (14a) by solving Eqs. (16a,b) in the absence of guiding ($R_m \to \infty$) and nonlinear focusing effects ($P_c \to \infty$). The solution of Eq. (16) in a uniform medium with refractive index η_p is

$$b(Z,\xi) = b_0(\xi) R^{-1}(Z,\xi) \left(\frac{1+\varepsilon^2(\xi)}{1+\varepsilon(\xi)(Z+\varepsilon(\xi))} \right)^{1/2} \exp\left(-\frac{\varepsilon(\xi)\alpha(\xi)}{1+\varepsilon^2(\xi)} Z \right), \tag{17a}$$

$$\varphi(Z,\xi) = -\tan^{-1}(Z+\varepsilon(\xi)) + \tan^{-1}(\varepsilon(\xi)) - \frac{\alpha(\xi)}{1+\varepsilon^2(\xi)} Z, \tag{17b}$$

$$\theta(Z,\xi) = \frac{-Z}{(1+\varepsilon(\xi)(Z+\varepsilon(\xi)))}, \tag{17c}$$

$$R(Z,\xi) = \left(\frac{1+(Z+\varepsilon(\xi))^2}{1+\varepsilon(\xi)(Z+\varepsilon(\xi))} \right)^{1/2}, \tag{17d}$$

and the wavefront radius of curvature is

$$R_c(Z,\xi) = R^2 Z_R / \theta(Z,\xi) = (Z_R/Z)\left(1+(Z+\varepsilon(Z,\xi))^2\right). \tag{17e}$$

In the paraxial limit, $\varepsilon(\xi) \to 0$, the functions b, φ, θ, R and R_c in Eqs. (17) reduce to the conventional expressions for the fundamental transverse Gaussian beam [26]

$$b(Z) = b_0 / R(Z) \tag{18a}$$

$$\varphi(Z) = -\tan^{-1} Z \tag{18b}$$

$$\theta(Z) = -Z, \tag{18c}$$

$$R(Z) = \left(1+Z^2\right)^{1/2}, \tag{18d}$$

$$R_c(Z) = (Z_R/Z)(1+Z^2). \tag{18e}$$

For propagation in vacuum we set $\eta_p = 1$ in Eqs. (17) and (18).

b) Group Velocity

To correctly obtain the group velocity it is necessary to use the quasi-paraxial wave equation in which finite pulse length effects are included. The paraxial wave equation in Eq. (11) does not contain finite pulse length effects; it is valid for infinitely long beams. Since Eq. (11) is independent of the variable ξ, which describes the pulse shape, finite pulse length effects can be included in an *ad hoc* manner by simply multiplying the paraxial solution by an arbitrary pulse envelope. In general, the group velocity is the velocity with which the peak of the pulse envelope travels, i.e., the velocity for which $\partial b(Z,\xi)/\partial\xi = 0$. In the paraxial approximation the group velocity is found to be $v_g = c\eta_p = c(ck/\omega)$ where we have taken the pulse amplitude to be $b_0(\xi) = \hat{b}_0 \exp(-4\xi^2/l_0^2)$ and $\hat{b}_0$ is the peak amplitude. In this approximation the product of the group and phase velocities is c^2.

In the quasi-paraxial approximation, which includes pulse length effects, from Eq. (17a) the pulse envelope can be written as

$$b(Z,\xi) = b_0(\xi)\left[1 - \varepsilon(\xi)Z/(1+Z^2)\right], \tag{19}$$

where b_0 is the amplitude in the paraxial approximation and the term proportional to ε is the QPA correction due to finite pulse length effects. Equation (19) is correct to order ε and is valid for $\varepsilon Z << 1$. In the presence of finite pulse length effects the group velocity is found to be

$$v_g(t) \approx c\eta_p\left[1 - \frac{1}{2}\left(\frac{\lambda}{\pi\eta_p r_0}\right)^2 \frac{\left(1 - c^2t^2/Z_R^2\right)}{\left(1 + c^2t^2/Z_R^2\right)^2}\right] \rightarrow c\eta_p\left[1 - \frac{1}{2}\left(\frac{\lambda}{\pi\eta_p r_0}\right)^2\right], \tag{20}$$

where the second expression is valid for $ct << Z_R$. In obtaining Eq. (20) we evaluated $\partial b/\partial\xi = 0$ in Eq. (19) and set $Z \approx ct/Z_R$ and $\xi = \int_0^t dt' v_g(t') - c\eta_p t$. When finite pulse length effects are properly included, as in the QPA, to lowest order in ε the group velocity is independent of the pulse length but depends on the spot size as given in Eq. (20).

IV. Coupled Envelope-Power Equations

In this section we analyze the propagation of a finite length laser pulse in a preformed plasma channel including nonlinear focusing effects. In general, for propagation in a plasma channel there is no equilibrium solution for a finite length high power laser pulse. For a sufficiently low power, where nonlinear focusing effects can be neglected, an equilibrium solution for finite length pulses exists. However, the equilibrium undergoes an envelope modulation. The normalized envelope equation for a laser pulse in a plasma channel, to first order in $\varepsilon(\xi)$, is obtained from Eqs. (14a,b)

$$\partial^2 R/\partial Z^2 - (1-P)R^{-3} + R_m^{-4}R + \varepsilon F(Z,\xi) = 0, \tag{21a}$$

where

$$P = P_0(\xi)\exp\left[-\varepsilon\int_0^Z G(Z',\xi)dZ'\right], \tag{21b}$$

is the normalized power,

$$F(Z,\xi) = R^{-2}\left[3 + (R/R_m)^4 - P + (R\partial R/\partial Z)^2\right]\partial R/\partial Z, \tag{21c}$$

$$G(Z,\xi) = R^{-2}\left[1 + (R/R_m)^4 + (R\partial R/\partial Z)^2\right], \tag{21d}$$

and $R = r_s/r_0$, $Z = z/Z_R$. In obtaining Eqs. (21) higher order finite length effects contained in α, which are of order ε^2, have been neglected. The coupled envelope-power equations for the guided pulse given by Eqs. (21) are nonlinear functions of spot size and contain finite pulse length effects. Several limiting cases, depending on the laser power and pulse duration will be discussed. In the following, low laser power refers to powers much less than the nonlinear focusing power, $P_L << P_c$.

a) Low power, Long pulse ($P << 1, \varepsilon = 0$),

In the low power, long pulse limit, the envelope equation reduces to

$$\frac{\partial^2 R}{\partial Z^2} + R_m^{-4} R - R^{-3} = 0. \tag{22}$$

The second term in Eq. (22) denotes plasma channel focusing while the last term represents diffraction. In this low power, long pulse limit, the beam has an equilibrium spot size $R_{eq} = R_m$.

b) Low power, Short pulse ($P << 1, \varepsilon \neq 0$),

In the low power, short pulse limit the equilibrium solution to Eqs. (16) is

$$R_{eq} = R_m, \tag{23a}$$

$$b_{eq}(Z,\xi) = b_0(\xi)\exp\left[-\varepsilon Z / R_m^2\right] \tag{23b}$$

$$\theta_{eq} = 0, \tag{23c}$$

$$\varphi_{eq}(Z) = -\frac{Z}{(1+\varepsilon^2)R_m^2}, \tag{23d}$$

while the equilibrium power is given by

$$P_{eq} = P_0 \exp[2\varepsilon\varphi_{eq}(Z)], \tag{23e}$$

and the pulse group velocity is given by the expression in Eq. (20). The effect of finite pulse length ($\varepsilon \neq 0$) is to make the peak of the pulse shift backward as the pulse propagates.

c) High power, Long pulse ($P \lesssim 1$, $\varepsilon = 0$)

In this limit, the equilibrium is given by

$$R_{eq}(\xi) = R_m\left(1 - P_{eq}(\xi)\right)^{1/4}, \tag{24a}$$

$$\theta_{eq} = 0, \tag{24b}$$

$$\varphi_{eq}(\xi, Z) = -\,(1 - P_{eq}/2)Z/R_{eq}^2, \tag{24c}$$

where $P_{eq} = P_0(\xi) = (P_{max}/P_c)\,(b_0(\xi)/\hat{b}_0)^2$ is the initial normalized laser power as a function of ξ. In this limit the laser power does not evolve with distance, i.e., $P_{eq} = P_0(\xi)$ is independent of Z. For peak laser powers less than the critical power, $P_0(\xi) < 1$, the equilibrium is stable.

In this limit for a uniform plasma (no channel guiding, $R_m = \infty$), a uniform laser beam i.e., independent of ξ, will have a longer Rayleigh length longer than the vacuum Rayleigh length because of nonlinear focusing effects. The modified Rayleigh length is given by

$$Z_R = (1 - P_{eq})^{-1/2} Z_{R0}, \tag{25}$$

provided $P_{eq} < 1$. For $P_{eq} > 1$, the beam focuses in a distance

$$L_f = (P_{eq} - 1)^{-1/2} Z_{R0}. \tag{26}$$

In Eqs. (25) and (26), Z_{R0} is the Rayleigh length associated with low power lasers, i.e., powers much less than the nonlinear focusing power ($P_{eq} << 1$).

d) High power, Short pulse ($P \lesssim 1$, $\varepsilon = 0$)

In this limit, the laser pulse does not have an equilibrium. The stability characteristics of laser pulses in plasma channels can be obtained by perturbing Eq. (21) about the spot size $R_{eq}(\xi) = R_m(1 - P_0(\xi))^{1/4}$, where $R = R_{eq} + \delta R$ and $|\delta R| << R_{eq}$. The equation for δR is

$$\partial^2 \delta R / \partial Z^2 + 4R_0^{-4}(1-P_0)\delta R + 4\varepsilon R_0^{-2}(1-P_0/2)\partial \delta R/\partial Z = -R_0^{-3}\delta P, \quad (27a)$$

where

$$\delta P = P_0\left(\exp\left[-\varepsilon(G_0 Z + \int_0^Z \delta G dZ')\right] - 1\right) \quad (27b)$$

$G_0 = 2R_0^{-1}(1 - P_0/2)$ and $\delta G = -2R_0^{-3}P_0\delta R$. Since there is no equilibrium for high power, short pulses propagating in a plasma channel, both the laser power and spot size evolve with propagation distance. The spatial evolution of the power and spot size, among other factors, is given by $\exp(-2\varepsilon(1-P_0/2)Z/R_0)$.

V. Laser Envelope Modulation

a) Envelope Oscillation

In the low power (P << 1), short pulse limit b) of the preceding section, the perturbed envelope equation is

$$\frac{\partial^2 \delta R}{\partial Z^2} + 4\delta R + 4\varepsilon \frac{\partial \delta R}{\partial Z} - 6\frac{c}{\omega}\frac{\partial^2 \delta R}{\partial \xi \partial Z} = 0, \quad (28a)$$

with solution

$$\delta R \approx \delta R_0 \exp(-2\varepsilon Z - Z^2/Z_d^2)\cos(2Z), \quad (28b)$$

where $\delta R_0 = \delta R(Z = 0)$, $\partial \delta R/\partial Z = 0$ at $Z = 0$ and $Z_d = \omega \ell_o /(2\sqrt{6}c)$ is the phase mixing length normalized to Z_R. The damping term is obtained from an extension of the QPA to include phase mixing. In obtaining the solution in Eq. (28b) it was assumed that the envelope period πZ_R is small compared to the growth length $Z_R/(2|\hat{\epsilon}|)$ and the phase mixing length $(\pi/6^{1/2})(\ell_0/\lambda)Z_R$ The modulation amplitude is proportional to

$$\exp[-8\lambda\xi Z/(\pi\eta_p \ell_o^2) - Z^2/Z_d^2]. \qquad (29)$$

The modulation at the front of the pulse ($\xi > 0$) is always damped while in the back ($\xi < 0$) it initially grows but is eventually damped due to frequency spread phase mixing. Overall damping of the modulation occurs for $Z > 2\pi|\xi|/(3\eta_p\lambda)$.

b) Laser Modulation Mechanism

The mechanism for the envelope modulation can be understood by noting the relationships between the group velocity, spot size and power of a pulse propagating in a plasma channel. The group velocity of a pulse in a plasma channel can be written as $v_g = v_{g0} + \delta v_g$, where the mean group velocity v_{g0} is given by Eq. (20), the perturbed group velocity is $\delta v_g = c(\lambda/\pi r_0)^2 \delta r/r_0$ and δr is the perturbed spot size. To lowest order, conservation of power implies $\delta b = - b_0 \delta r/r_0$, where δb and b_0 are the perturbed and unperturbed laser field amplitudes, respectively. Figure 1(a,b) shows the amplitude and spot size of a finite pulse length laser in a reference frame moving with the mean group velocity v_{g0}. The solid curve shows the equilibrium amplitude and spot size as a function of $z - v_{g0}t$. If the spot size is uniformly increased ($\delta r > 0$) along the pulse, the group velocity increases by the amount δv_g. The amplitude in front of the unperturbed pulse increases ($\delta b > 0$) while the amplitude in back of the unperturbed pulse decreases ($\delta b < 0$). Conservation of power indicates that the perturbed spot

size in back of the pulse is further increased since $\delta r = - r_0 \delta b/b_0 > 0$ and decreased in front of the pulse since $\delta r = - r_0 \delta b/b_0 < 0$. If, instead, initially the spot size were uniformly decreased, the spot size at the back would be further decreased while in the front it would increase. Hence, the perturbed spot size is damped in front of the pulse and is unstable in the back. Substituting $\xi = z - v_g t = z - v_{g0} t - \delta v_g t = \xi_0 - \delta v_g t$ into $b \sim b_0 \exp(-4\xi^2/\ell_0^2)$, the rate of change of the perturbed amplitude is $\partial \delta b / \partial t \approx 8 b_0 \xi_0 \delta v_g / \ell_0^2$. Using $\delta r = -(r_0/b_0)\delta b$, we find $\partial \delta r / \partial t = -8c\xi_0 (\lambda/\pi r_0)^2 \delta r / \ell_0^2$ which agrees with the growth term in Eq. (29). Inherent to a finite laser pulse is a frequency spread given by $\delta\omega \sim c/\ell_0$. Hence the envelope modulation frequency $\Omega_e = 2c/Z_R$ acquires a spread $\delta\Omega_e \sim \Omega_e \, \delta\omega/\omega \sim \Omega_e (\lambda / 2\pi\ell_o)$. This envelope frequency spread results in phase mixing of the modulation in a distance Z_d (normalized to Z_R).

VI. Numerical Illustrations

Figure 2 is a plot of the normalized spot size $R(Z,\xi)$ in Eq. (17d) as a function of ξ for various values of $Z = 0, 1, 2, 3$. In this figure the laser pulse propagates in vacuum and the pulse length is $\ell_0 = 6\ \lambda$. In the absence of finite length effects the spot size would be independent of ξ. Figure 2 indicates that the tail of the pulse flares out more than the front of the pulse, leading to a "trumpet" pulse shape.

In Figs. 3-6 the laser pulse parameters are $\lambda = 1$ μm, $\omega_p/\omega << 1$ $\ell_0 = 20$ μm (67 fs) and the peak power is $P_{peak} = 0.56\ P_c$. The total nonlinear focusing power, P_c, is given by Eq. (4c) and consists of contributions from free and atomic electrons. In all the figures there is an initial

mismatch in the spot size compared to the equilibrium spot size, i.e., $R_0 = R(0,0) = 1$ and $R_m = 1.15$. Figure 3(a) shows the spot size $R(Z,\xi)$ as a function of $Z = z/Z_R$ and ξ/λ, with finite pulse length effects ($\varepsilon \neq 0$) included. For comparison Fig. 3(b) shows the same plot except in the absence of finite length effects ($\varepsilon = 0$). The laser envelope modulation is clearly seen in Fig. 3(a) where the spot size oscillations at the front of the pulse ($\xi > 0$) are damped and in the back ($\xi < 0$) grow. Finite pulse effects not only result in an envelope modulation but also significantly enhance nonlinear focusing. This is shown in Fig. 4 where the spot size with finite pulse length effects (solid curve) approaches zero at $\xi/\lambda = -3$ for $Z = 15$. The spot size without finite length effects (dotted curve) shows less than a 10% decrease at $\xi \approx 0$ for $Z = 15$. Figures 5(a) and (b) show the laser pulse amplitude $b(Z,\xi)$ as a function of Z and ξ/λ with and without finite pulse length effects, respectively. As a result of the enhanced nonlinear focusing due to the finite pules length, Fig. 5(a) shows a significant increase in the pulse amplitude at $Z = 15$ compared to Fig. 5(b). Figure 6 shows the pulse power as a function of ξ/λ and radial coordinate r/r_0 at $Z = 15$. Finite length effects in Fig. 6(a) result in an increase in the peak power as well as a distortion of the pulse compared to Fig. 6(b), where finite length effects are absent. In Fig. 6(a), finite length effects reduce the pulse propagation velocity, i.e., peak of the pulse occurs at negative values of ξ. In Fig. 6(b), nonlinear focusing effects are included while finite pulse length effects are neglected, $\varepsilon = 0$. For $\varepsilon = 0$ the pulse velocity is c and nonlinear focusing is substantially reduced.

VII. Conclusions

The increasing use of ultra short laser pulses in many applications requires that the paraxial wave equation be extended to include finite pulse length effects. We present the quasi

paraxial approximation (QPA) to the wave equation. The QPA is an extension of the usual paraxial approximation and takes finite pulse length effects into account. A pair of coupled envelope-power equations is derived for short laser pulses propagating in vacuum, plasmas and preformed plasma channels. The model includes atomic electron and relativistic effects. We find that finite length effects can significantly modify the laser field. The new results include: i) an analytical formulation of short laser pulses, ii) a derivation of a pair of coupled laser envelope-power equations, iii) a laser envelope modulation, iv) demonstration of significant modification of nonlinear processes by finite pulse length effects, and v) analysis of short pulse propagation dynamics in long plasma channels.

Appendix: Validity of the Quasi Paraxial Approximation

The approximation, which leads to the simplified wave equation in Eq. (14a), requires that

$$|\varepsilon\, \mathbf{E}_0| >> \left| \left(\varepsilon + \frac{c}{\eta_p \omega} \frac{\partial}{\partial \xi} \right) \mathbf{E}_0 \right|, \tag{A1}$$

where E_0 and ε are given by Eq. (13) and (14b). The short pulse approximation requires that Eq. (A1) be satisfied.

a) Approximation in Vacuum

For pulse propagation in vacuum, $\eta_p = 1$, the inequality in Eq. (A1) can be rewritten and the approximation is shown to be valid if

$$|\xi| >> \frac{\lambda}{2\pi} \left| \frac{Z}{1 + i(Z + \varepsilon)} \right| \left| 1 + \frac{(r/r_0)^2}{1 + i(Z + \varepsilon)} \right|, \tag{A2}$$

where we have assumed $|\varepsilon| << 1$. The finite pulse length approximation in vacuum, used to replace $\partial \mathbf{E}_0 / \partial \xi$ with $-(\omega/c)\varepsilon(\xi)\mathbf{E}_0$ in Eq. (14a), is well satisfied everywhere except within a small function of a wavelength of the pulse's center.

b) Approximation in Guiding Channel

To determine the validity of the short pulse approximation in a guiding channel we consider the low power, short pulse limit of Eq. (21), i.e., limit b) in Sec. IV. The field in Eq. (13) for the equilibrium solution given in Eqs. (23) is

$$\mathbf{E}_{eq} = b_0(\xi) \exp\left[-\varepsilon Z / R_m^2 - i r^2 / (r_0 R_m)^2 \right]. \tag{A3}$$

Substituting $\mathbf{E}_{eq}$ for $\mathbf{E}_0$ in Eq. (A1) yields the condition for the QPA to be valid. The approximation is valid provided $|\varepsilon| >> (c/\omega\eta_p)|\partial\varepsilon/\partial\xi|Z/R_m^2$, which for a pulse having a Gaussian longitudinal profile is

$$|\xi| >> \frac{1}{\eta_p}\frac{\lambda}{2\pi}R_m^{-2}Z. \tag{A4}$$

The QPA approximation is not valid for long propagation distances.

Acknowledgment

The authors acknowledge discussions with R.F. Hubbard, A. Ting, A. Zigler and acknowledge the assistance of J. Penano in preparing the computer graphics. This work was supported by the Office of Naval Research and the Department of Energy.

References

1. G.A. Mourou, C.P.J. Barty, and M.D. Perry, Phys. Today **51**, 22 (1998).
2. C.P.J. Barty, Laser Focus World, June issue, 93 (1996).
3. M.D. Perry and G. Mourou, Science **264,** 917 (1994).
4. P. Sprangle, E. Esarey, and J. Krall, Phys. Plasmas **3**, 2183 (1996).
5. E. Esarey, P. Sprangle, J. Krall, and A. Ting, IEEE Trans. Plasma Sci. **24**, 252 (1996).
6. J.A. Edighoffer and R.H. Pantell, J. Appl. Phys. **50**, 6120 (1979).
7. Y.C. Huang, D. Zheng, W.M. Tulloch, and R.L. Byer, Appl. Phys. Lett. **68**, 753 (1996); Y.C. Huang and R. L. Byer, *ibid.* **69**, 2175 (1996).
8. P. Sprangle, E. Esarey, J. Krall, and A. Ting, Opt. Commun. **124**, 69 (1996).
9. E. Esarey, P. Sprangle, and J. Krall, Phys. Rev. E **52**, 5443 (1995).
10. B. Hafizi, A. Ting, E. Esarey, P. Sprangle, and J. Krall, Phys. Rev. E **55**, 5924 (1997); B. Hafizi, E. Esarey and P. Sprangle, Phys. Rev. E **55**, 3539 (1997).
11. K. Nakajima, D. Fisher, T. Kawakubo, H. Hashaniki, A. Ogata, Y. Kato, Y. Kitagawa, R. Kodama, K. Mima, H. Shiraga, K. Suzuki, K. Yamakawa, T. Zhang, Y. Sakawa, T. Shoji, Y. Nishida, N. Yagami, M. Downer, and T. Tajima, Phys. Rev. Lett. **74** 4659 (1995).
12. C.E. Clayton, K.A. Marsh, A. Dyson, M. Everett, A. Lal, W.P. Leemans, R. Williams, and C. Joshi, Phys. Rev. Lett. **70**, 37 (1993); C.E. Clayton, M.J. Everett, A. Lal, D. Gordon, K.A. Marsh, and C. Joshi, Phys. Plasmas **1**, 1753 (1994); A. Modena, Z. Najmudin, A.E. Dangor, C.E. Clayton, K.A. Marsh, C. Joshi, V. Malka, C.B. Darrow, and C. Danson, IEEE Trans. Plasma Sci. **PS-24**, 289 (1996).
13. D. Umstadter, S.Y. Chen, A. Maksimchuk, G. Mourou, and R. Wagner, Science **273**, 472 (1996).

14. A. Ting, C.I. Moore, K. Krushelnick, C. Manka, E. Esarey, P. Sprangle, R. Hubbard, H.R. Burris, and M. Baine, Phys. Plasmas **4**, 1889 (1997); C.I. Moore, A. Ting, K. Krushelnick, E. Esarey, R.F. Hubbard, B. Hafizi, H.R. Burris, C. Manka, and P. Sprangle, Phys. Rev. Lett. **79**, 3909 (1997).

15. J. Zhou, J. Peatross, M.M. Murnane, H.C. Kapteyn, and I.P. Christov, Phys. Rev. Lett. **76**, 752 (1996).

16. H.M. Milchberg, C.G. Durfee III, and T.J. MacIlrath, Phys. Rev. Lett. **75**, 2494 (1995).

17. P. Sprangle and E. Esarey, Phys. Rev. Lett. **67** 2021 (1991).

18. E. Esarey and P. Sprangle, Phys. Rev. A. **45**, 5872 (1992).

19. E. Esarey, A. Ting, P. Sprangle, D. Umstadter, and X. Liu, IEEE Trans. Plasma Sci. **21**, 95 (1993).

20. D.C. Eder, P. Amendt, L.B. DaSilva, R.A. London, B.J. MacGowan, D.L. Matthews, B.M. Penetrante, M.D. Rosen, S.C. Wilks, T.D. Donnelly, R.W. Falcone, and G.L. Strobel, Phys. Plasmas **1**, 1744 (1994).

21. S. Suckewer and C.H. Skinner, Comments At. Mol. Phys. **30**, 331 (1995).

22. B.E. Lemoff, G.Y. Yin, C.L. Gordon III, C.P.J. Barty, and S.E. Harris, Phys. Rev. Lett. **74** 1574 (1995).

23. M. Tabak, J. Hammer, M.E. Glinsky, W.L. Kruer, S.C. Wilds, J. Woodworth, E.M. Campbell, M.C. Perry, and R.J. Mason, Phys. Plasmas **1**, 1626 (1994).

24. C. Deutsch, H. Furukawa, K. Mima, M. Murakami, and K. Nishihara, Phys. Rev. Lett. **77** 2483 (1996).

25. R. Kodama, K. Takahashi, K.A. Tanaka, M. Tsukamoto, H. Hashimoto, Y. Kato, and K. Mima, Phys. Rev. Lett. **77** 4906 (1996).

26. A.E. Siegman, *Lasers* (University Science Books, Mill Valley, CA, 1986).

27. E. Esarey, P. Sprangle, M. Pilloff, and J. Krall, J. Opt. Soc. Am. B **12**, 1695 (1995).

28. M. Borghesi, A.J. McKinnon, L. Barringer, R. Gaillard, L.A. Gizzi, C. Meyer, O. Willi, A. Pukhov, and J. Meyer-ter-Vehn, Phys. Rev. Lett **78**, 379 (1996).

29. M. Borghesi, A.J. Mackinnon, R. Gaillard, O. Willi, and A.A. Offenberger, Phys. Rev. E **57**, R4899 (1998).

30. A. Braun, G. Korn, X. Liu, D. Du, J. Squier, and G. Mourou, Opt. Lett **19** 1544 (1995).

31. H.R. Lange, G. Grillon, J.-F. Ripoche, M.A. Franco, B. Lamouroux, B.S. Prade, A. Mysyrowicz, E.T.J. Nibbering, and A. Chiron, Opt. Lett. **23**, 120 (1998).

32. P. Sprangle, E. Esarey, and J. Krall, Phys. Rev. E **54,** 4211 (1996).

33. C.G. Durfee III, T.R. Clark, and H.M. Milchberg, J. Opt. Soc. Am. B **13**, 59 (1996).

34. H.M. Milchberg, T.R. Clark, C.G. Durfee III, T.M. Antonsen, and P. Mora, Phys. Plasmas **3**, 2149 (1996).

35. T.R. Clark and H.M. Milchberg, Phys. Rev. Lett. **78**, 2773 (1997).

36. K. Krushelnick, A. Ting, C.I. Moore, H.R. Burris, E. Esarey, P. Sprangle, and M. Baine, Phys. Rev. Lett. **78**, 4047 (1997).

37. A. Zigler, Y. Ehrlich, C. Cohen, J. Krall, and P. Sprangle, J. Opt. Soc. Am. B **13** 68 (1996).

38. Y. Ehrlich, C. Cohen, A. Zigler, J. Krall, P. Sprangle, and E. Esarey, Phys. Rev. Lett. **77**, 4186 (1996).

39. D. Kaganovich, P.V. Sasarov, Y. Ehrlich, C. Cohen, and A. Zigler, Appl. Phys. Lett. **71**, 2295 (1997).

40. Y. Ehrlich, C. Cohen, D. Kaganovich, A. Zigler, R.F. Hubbard, P. Sprangle, and E. Esarey, J. Opt. Soc. Am. B **15**, 2416 (1998).

41. X.L. Chen and R.N. Sudan, Phys. Fluids B **5**, 133 (1993).

42. W.B. Mori, C.D. Decker, D.E. Hinkel, and T. Katsouleas, Phys. Rev. Lett. **72**, 1482 (1994).

43. C.D. Decker, W.B. Mori, and T. Katsouleas, Phys. Rev. E **50**, R3338 (1994).

44. P. Mora and T.M. Antonsen, Phys. Plasmas **4**, 217 (1997).

45. P. Sprangle, E. Esarey, and B. Hafizi, Phys. Rev. Lett. **79**, 1046 (1997).

46. P. Sprangle, E. Esarey, and B. Hafizi, Phys. Rev. E **56**, 5894 (1997).

47. C.E. Max, J. Arons, and A.B. Langdon, Phys. Rev. Lett. **33**, 209 (1974).

48. A.G. Litvak, Zh. Eksp. Teor. Fiz. **57**, 629 (1969) [Sov. Phys. JETP **30**, 344 (1969)].

49. P. Sprangle, C.M. Tang, and E. Esarey, IEEE Trans. Plasma Sci. **15**, 145 (1987).

50. G. Schmidt and W. Horton, Comments Plasma Phys. Control. Fusion **9**, 85 (1985); G.Z. Sun, E. Ott, Y.C. Lee, and P. Guzdar, Phys. Fluids **30**, 526 (1987); A.B. Borisov, A.V. Borovskiy, O.B. Shiryaev, V.V. Korobkin, A.M. Prokhorov, J.C. Solem, T.S. Luk, K. Boyer, and C.K. Rhodes, Phys. Rev. A **45** 5830 (1992).

51. J.F. Reintjes, *Nonlinear Optical Parametric Processes in Liquids and Gases* (Academic, Orlando, FL, 1984).

52. Y.R. Shen, *The Principles of Nonlinear Optics*, (Wiley, New York, 1984).

53. R.W. Boyd, *Nonlinear Optics* (Academic, San Diego, 1993).

54. P. Sprangle, E. Esarey, and A. Ting, Phys. Rev. Lett. **64**, 2011 (1990).

55. P. Sprangle, E. Esarey, A. Ting, and G. Joyce, Appl. Phys. Lett. **53**, 2146 (1988).

56. K.C. Tzeng, W.B. Mori, and T. Katsouleas, Phys. Rev. Lett. **79**, 5258 (1997).

57. Note that simply equating powers of r in Eq. (14a) results in critical powers that are small by a factor of 2. Equation (16) is obtained by a more proper approach using the source dependent expansion method, P. Sprangle, A. Ting and C.M. Tang, Phys. Rev. Lett. **59**, 202 (1987); Phys, Rev. A**36**, 2773 (1987).

Figure Captions

Fig. 1 Illustration of the physical mechanism for the laser envelope modulation. The amplitude is shown in (a) and the spot size in (b), as a function of $\xi_0 = z - v_{g0}t$, where v_{g0} is the mean group velocity. The solid curves correspond to the equilibrium. The dashed curves show the amplitude and spot size for the case with group velocity larger than v_{g0} (1) and the case with group velocity smaller than v_{g0} (2).

Fig. 2 Plot of normalized spot size R(Z,ξ) as a function of ξ for a pulse of length $\ell_0 = 6\lambda$ propagating in free space. The four curves correspond to normalized axial points Z = 0 (lowest curve), 1,2, and 3.

Fig. 3 Surface plots of spot size R as a function of ξ/λ and propagation distance $Z = z/Z_R$ with (a) finite pulse length effects $(\varepsilon \neq 0)$ and (b) finite pulse length effects neglected $(\varepsilon = 0)$. The parameters are $\lambda = 1\mu m$, $\ell_0 = 20\mu m$, $P_{peak} = 0.56P_c$.

Fig. 4 Plot of spot size R as a function of ξ/λ after a propagation distance equal to 15 Rayleigh lengths $(Z = 15)$. The solid (dotted) curve includes (neglects) finite pulse length effects. Parameters are the same as in Fig. 3.

Fig. 5 Surface plots of laser pulse amplitude b as a function of ξ/λ and propagation distance $Z = z/Z_R$ with (a) finite pulse length effects $(\varepsilon \neq 0)$ and (b) finite pulse length effects neglected $(\varepsilon = 0)$. Parameters are the same as in Fig. 3.

Fig. 6 Surface plots of laser pulse power P as a function of ξ/λ and radial coordinate r/r_0 after a propagation distance equal to 15 Rayleigh lengths (Z = 15). In (a) finite pules length effects are included and show enhanced focusing and decreased propagation velocity, i.e.,

peak of the pulse occurs for negative values of ξ. In (b) finite pulse length effects are neglected, i.e., $\varepsilon = 0$ while nonlinear focusing effects are included. Parameters are the same as in Fig. 3.

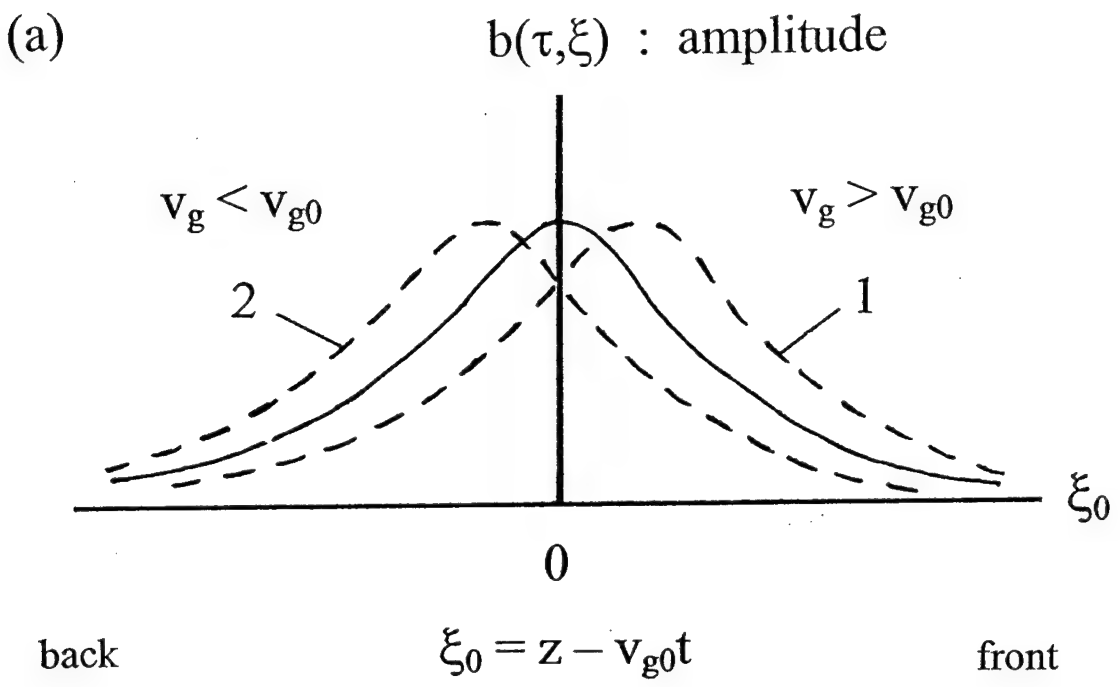
(a)
b(τ,ξ) : amplitude
$v_g < v_{g0}$
$v_g > v_{g0}$
2
1
ξ_0
0
back
$\xi_0 = z - v_{g0}t$
front

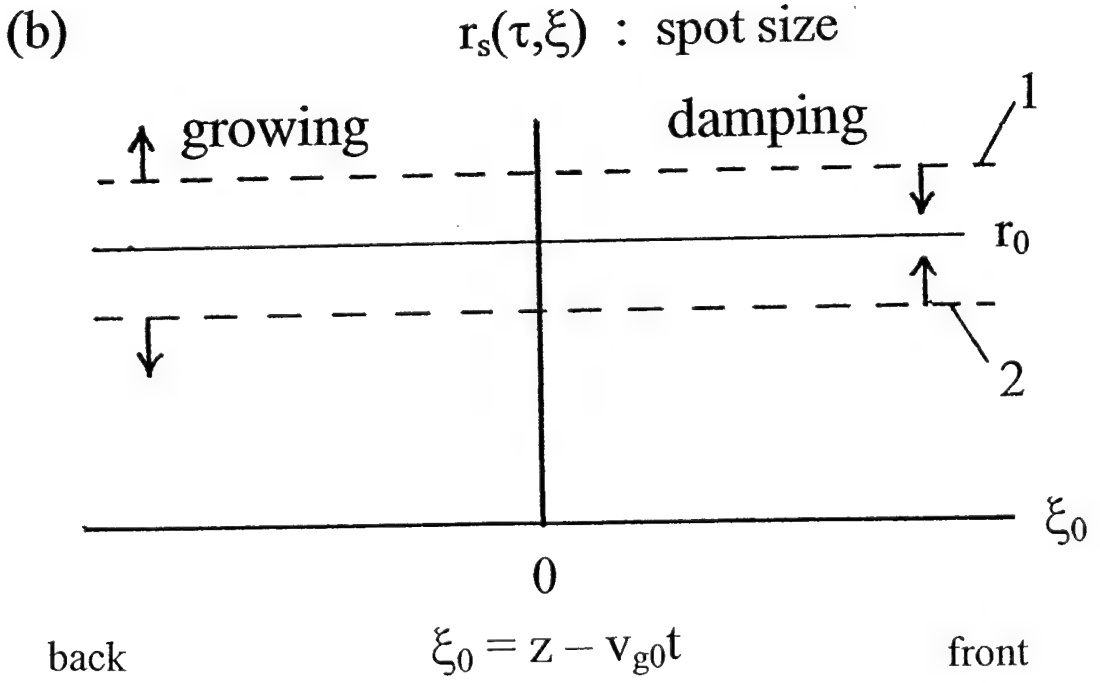
(b)
$r_s(\tau,\xi)$: spot size
growing
damping
1
r_0
2
ξ_0
0
back
$\xi_0 = z - v_{g0}t$
front

Fig. 1

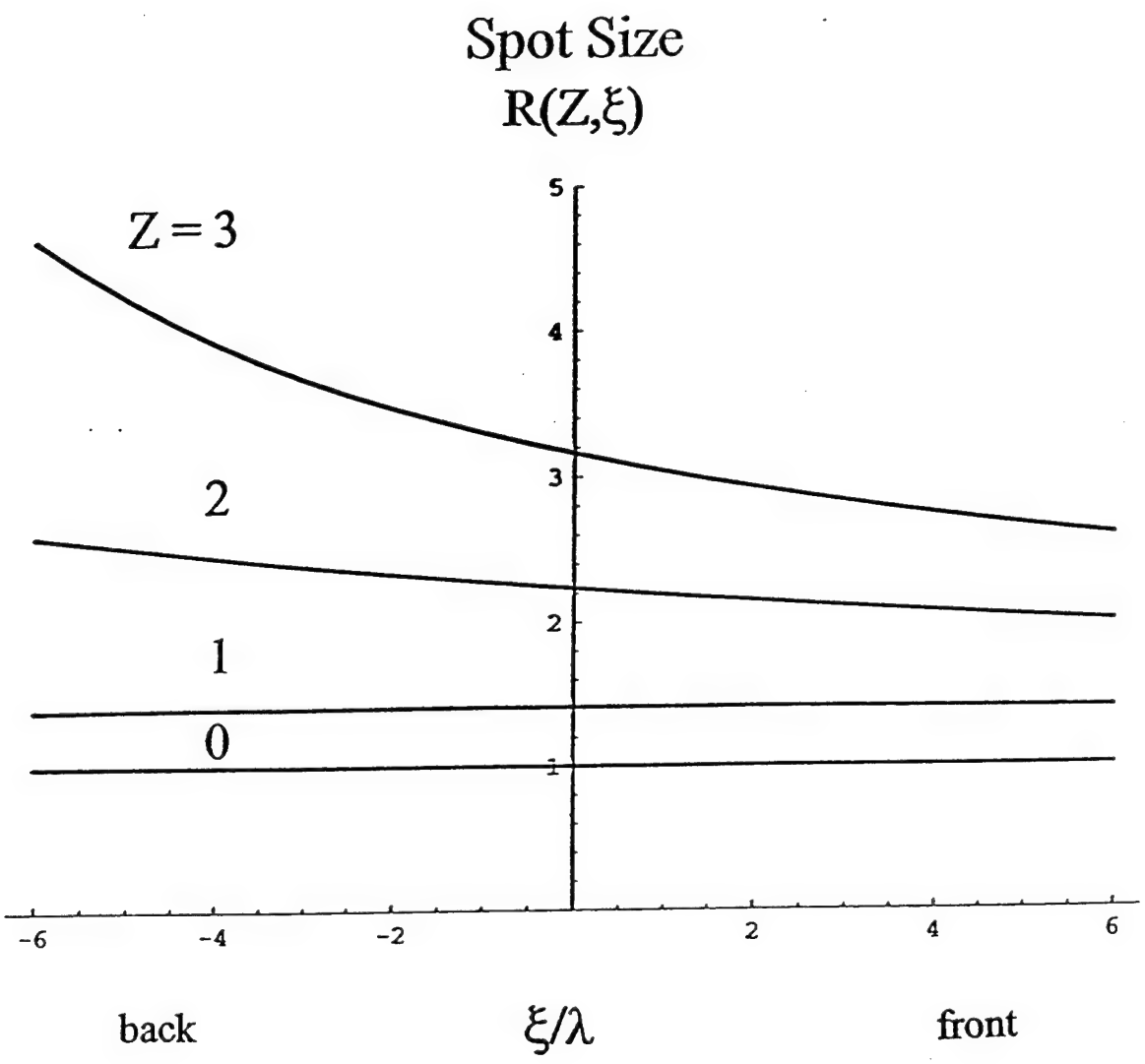

Fig. 2

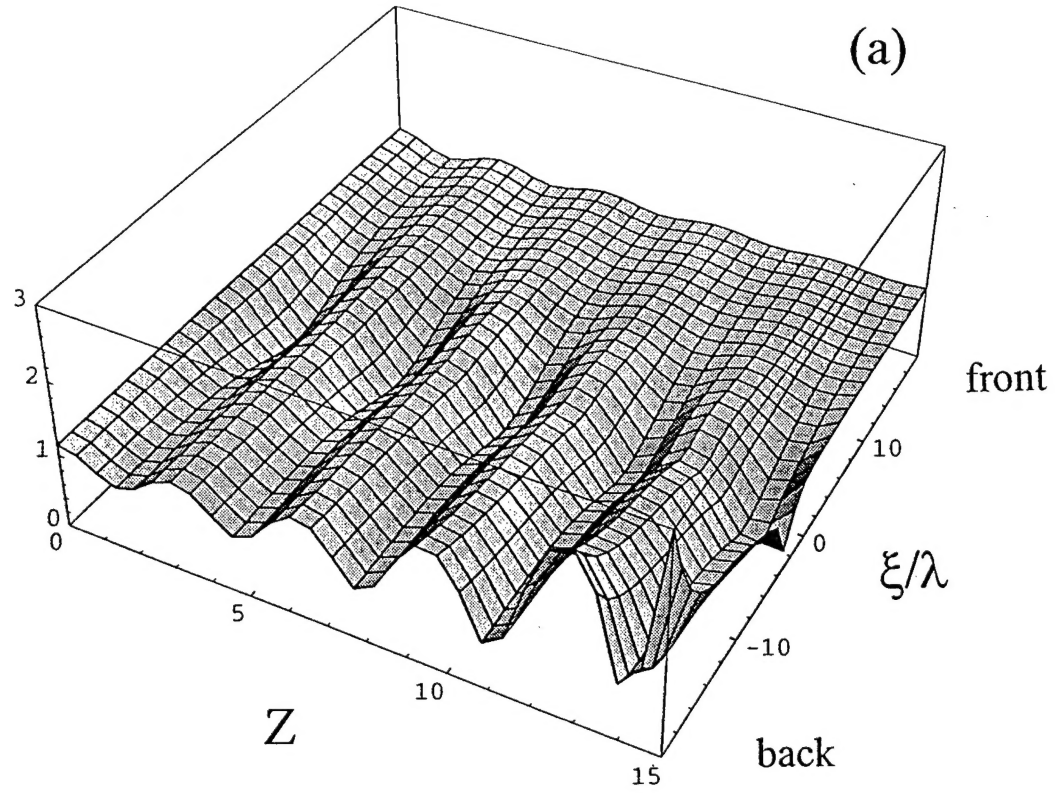
(a)
Spot Size
R(Z,ξ)
3
2
1
0
0
5
10
15
Z
front
10
0
-10
ξ/λ
back

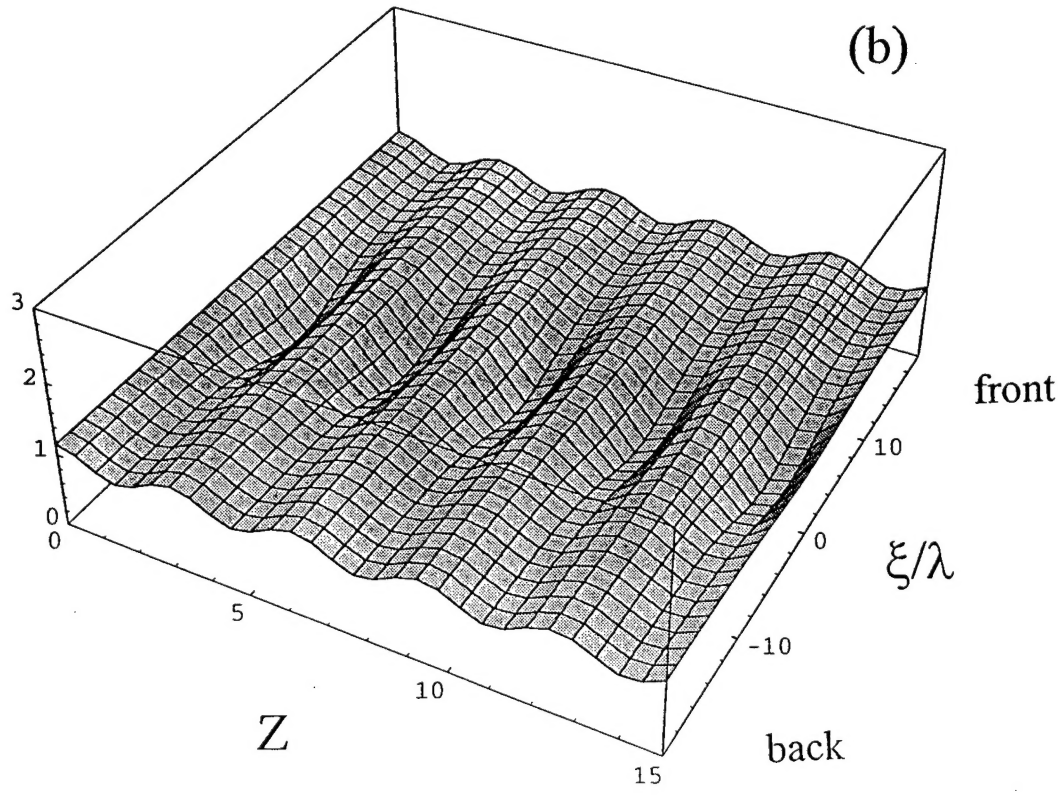
(b)
Spot Size
R(Z,ξ)
3
2
1
0
0
5
10
15
Z
front
10
0
-10
ξ/λ
back

Fig. 3

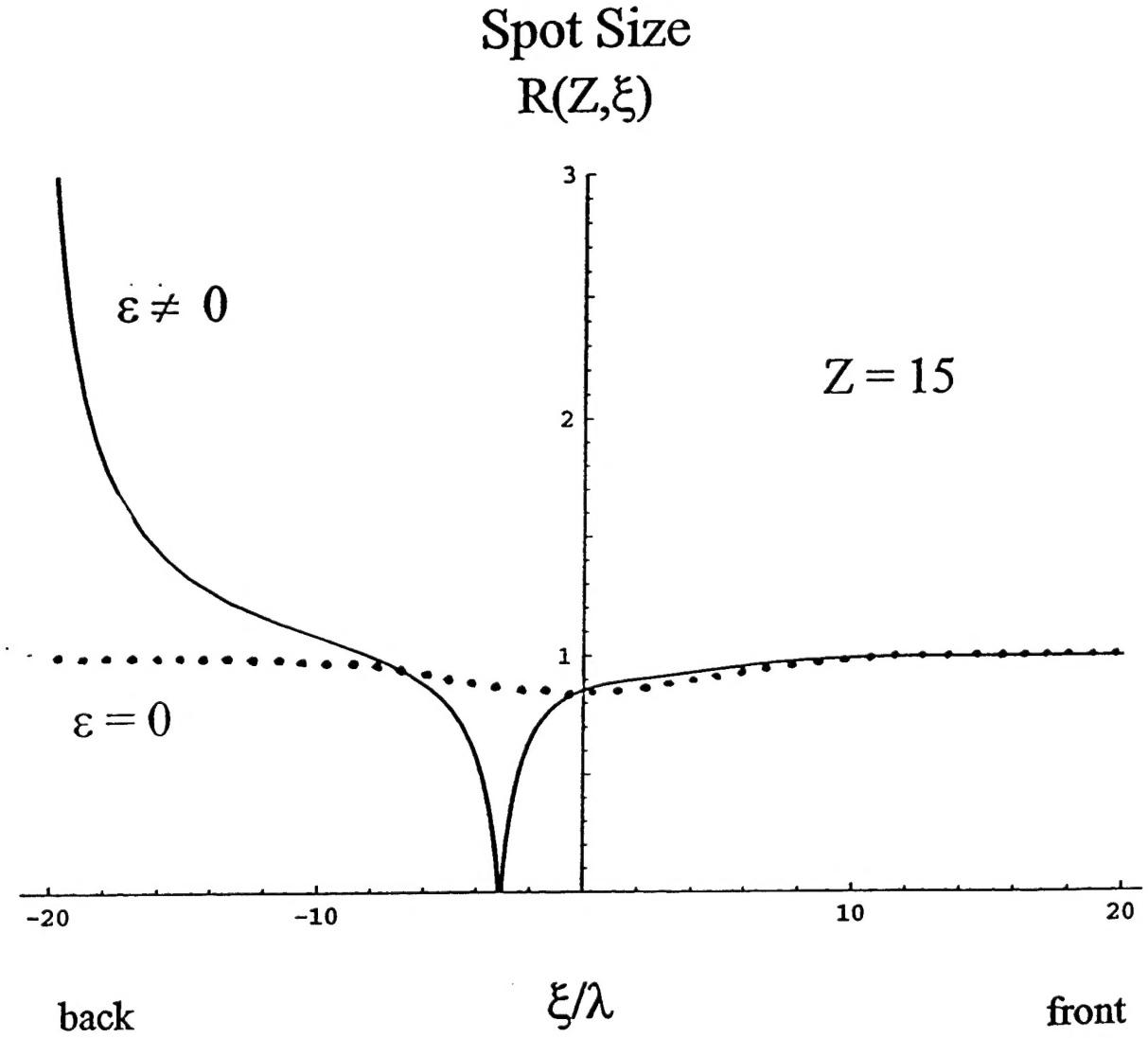

Fig. 4

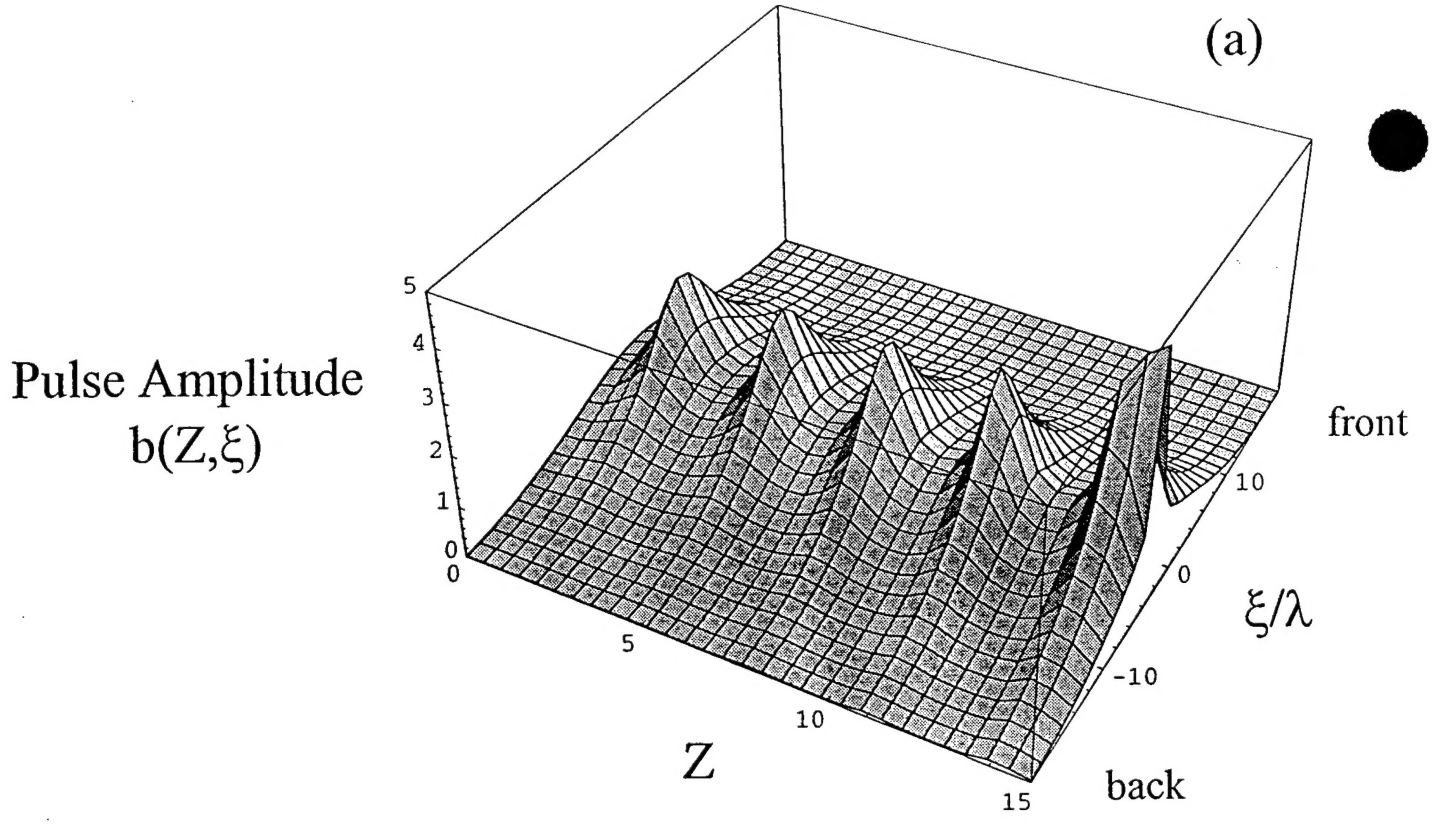
(a)
Pulse Amplitude
b(Z,ξ)
5
4
3
2
1
0
0
5
10
15
Z
front
10
0
-10
ξ/λ
back

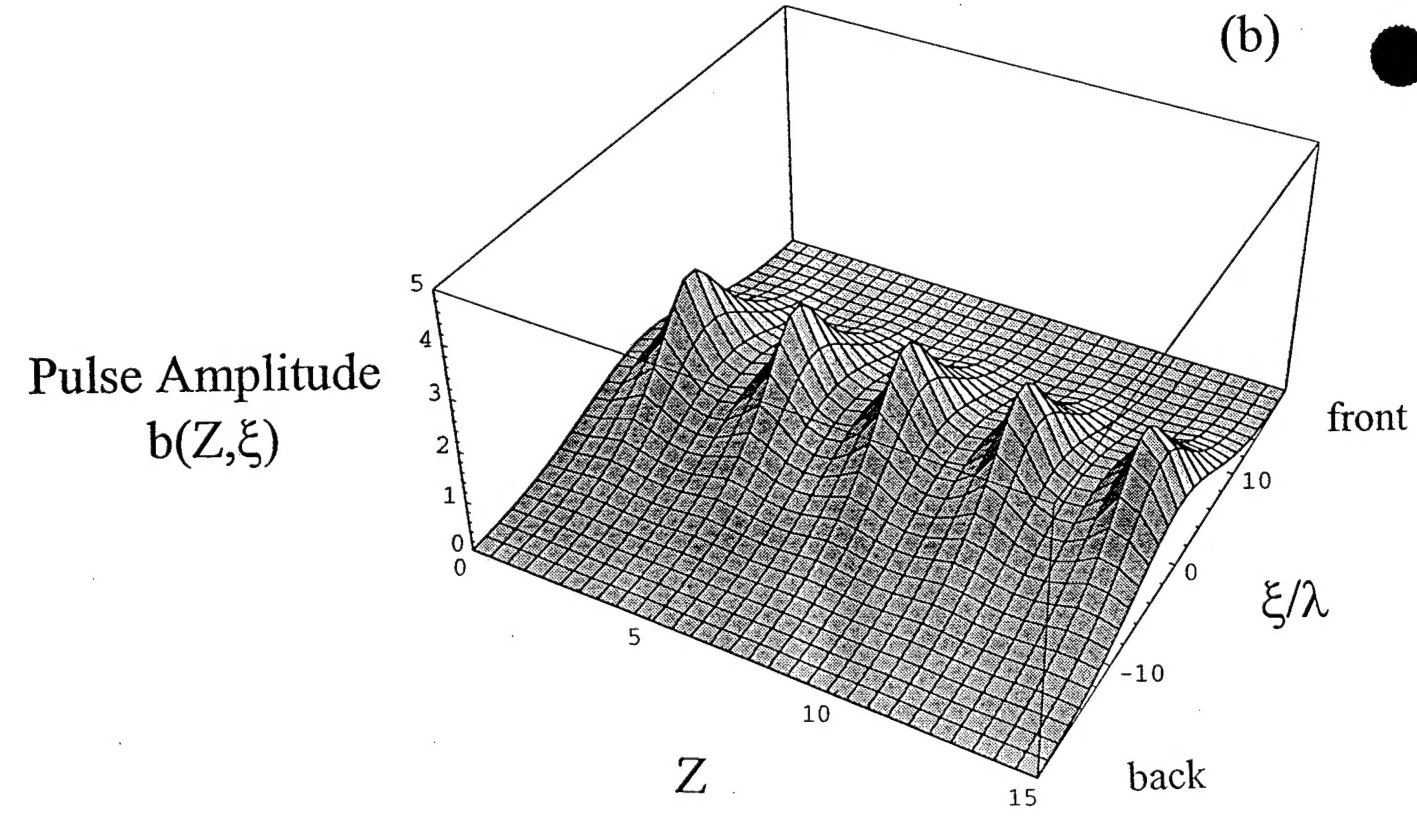
(b)
Pulse Amplitude
b(Z,ξ)
5
4
3
2
1
0
0
5
10
15
Z
front
10
0
-10
ξ/λ
back

Fig. 5

(a)

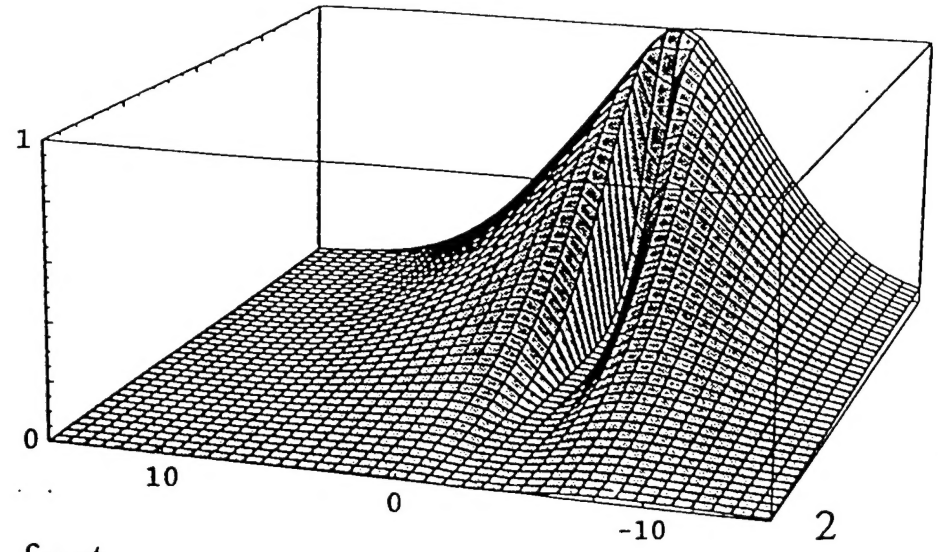
Power
P(Z,ξ)
1
0
10
0
-10
2
0
r/r0
front
ξ/λ
back

(b)

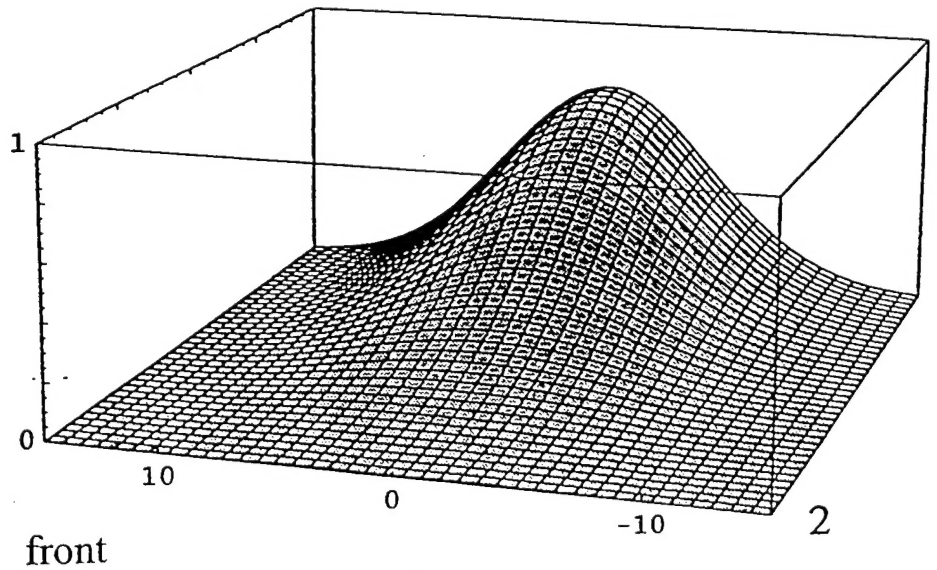
Power
P(Z,ξ)
1
0
10
0
-10
2
0
r/r0
front
ξ/λ
back

Fig. 6